Title: Evidence of Matuyama-Brunhes transition in the cave sediment in Central Europe

Hakan Ucar[1*], Gunther Kletetschka[1,2,3], Jaroslav Kadlec[4]

[1]Faculty of Science, Charles University, Prague, Czech Republic, [2]The Czech Academy of Sciences, Institute of Geology, Czech Republic [3]Geophysical Institute, University of Alaska Fairbanks, AK, USA, [4]Institute of Geophysics, Czech Academy of Sciences, Czech Republic.

*Corresponding author: ucarh@natur.cuni.cz

Co-author's emails: gunther.kletetschka@natur.cuni.cz; kadlec@ig.cas.cz

Abstract

In this study, we identified the Matuyama-Brunhes magnetic reversal recorded in cave sediments in Central Europe, Czech Republic. We collected discrete samples from the homogeneous sedimentary profile in the Za Hajovnou cave located in the eastern part of the Czech Republic. Novel use of characteristic remanent magnetization (ChRM) directions and VGP path of the data revealed Matuyama-Brunhes transition boundary within 5 cm of the Za Hajovnou cave sediment. This result revealed a new more detailed behavior of the polarity transition from the central European location. Migration of the paleopole between east of Africa and west of North America is a significant marker in terms of the central European paleomagnetic record. Also we estimated the sedimentation rate of the cave. In addition, we discussed our results with a supporting data associated with tektites in the light of a new hypothesis that a meteorite impact could be a reason of Matuyama-Brunhes reversal.

Keywords: Matuyama-Brunhes, paleomagnetism, magnetic reversal, cave, sediments, meteorite impact

1. Introduction

Matuyama-Brunhes magnetic reversal occured approximately 781 kyr ago (Lourens et al., 2004). Studies in recent years (Channel et al., 2010; Giaccio et al., 2013; Jin and Liu, 2011;

Kitaba et al., 2013; Liu et al., 2016; Okada et al., 2017; Pares et al., 2016; Sagnotti et al., 2010, 2014; Suganuma et al., 2010; Valet et al., 2014; Bella et al., 2019) have shown that this event is well recorded by respective sediments that had sufficient sedimentation rate and could be analyzed, in detail, by paleomagnetism.

Sediments acquire remanent magnetization during their deposition. The alignment of ferromagnetic grains occurs in the direction of the earth's magnetic field and acquisition of primary magnetization due to this sedimentation process is called depositional or detrital remanent magnetization (DRM) (Gubbins and Herrero, 2017). Remanent magnetization protected by energy barriers can last over geologic time scales. Nevertheless, due to thermal and/or chemical processes such as reheating, oxidation and formation of iron hydroxides during time, barriers may be overcome, the magnetic domains change their arrangement and rocks can acquire secondary magnetizations. The new secondary magnetization has an orientation in the direction of the Earth's field. Then rocks can acquire a viscous magnetization (VRM) long time after their formation due to an exposure to geomagnetic field. VRM contrinutes to a noise in paleomagnetic data (Lanza and Meloni, 2005; Butler, 1997).

Lock-in-depth affects the nature of the paleomagnetic recording process in sediments. It is defined as the depth at which the remanent magnetization is stabilized. Lithology, grain-size distribution of the sediment matrix, sedimentation rate and bioturbation, all have influence on the position of the lock-in-depth in the sediments (Sagnotti et al., 2005; Bleil and von Dobeneck, 1999). When assuming the steady sedimentation rate, the result of lock-in-depth stabilization is younger magnetization than the sediment itself by an amount of time required to accumulate sediment layer of thickness that equal to the lock-in-depth. For example, if the sediment has accumulation speed 1 mm per 1000 years, and lock-in-depth is 10 mm, the magnetization age is 10 000 years younger than the sediment itself (Sagnotti et al., 2005).

Kadlec et al. (2005, 2014) reported that the Central European cave (local name "Za Hajovnou"), in the Moravia region of the Czech Republic, has a potential record of Matuyama-Brunhes transition. Here we obtained a new paleomagnetic dataset from three vertical sediment profiles found in this cave.

1.1 Geology and Sampling

The Za Hájovnou Cave (49° 40′ N, 16° 55′E) is a former sinkhole located in Javoricko Karst, Moravia Region of the Czech Republic (Lundberg et al., 2014; Musil, 2014) (Figure 1). The Javoricko Karst is formed by light-grey-coloured massive Devonian limestone that overlies Pre-Cambrian phyllite (Lundberg et al., 2014; Musil, 2014). Spranek and Javoricka are two rivers that flow through the Jarovicko karst. While Za Hájovnou Cave is situated on the north-western bank of the Javoříčka river on the southern slope of a Pani Hora hill (Lundberg et al., 2014; Musil, 2014; Zak et al., 2018;), both Spranek and Javoricka watershed may have contributed to the sediment development in this cave (Figure 1).

The Za Hajovnou cave is approximately 500 m long system (Babek et al., 2015; Musil, 2005). The cave's corridors were expored previously in a total length of ~200 m (Musil, 2014) (Figure 2). The cave currently consists of two main parallel corridors with slightly different sedimentological record (Musil et al., 2014); the first corridor (local name is "Excavated Corridor") used to be sinkhole entrance) and the other corridor (local name is "Birthday Corridor") has separate entrance and is connected with the Excavated Corridor by the Connecting Passage Corridor (Figure 2). Sediments from the Excavated Corridor continue to Birthday Corridor and partially filled the Connecting Passage Corridor (Musil et al., 2014) (Figure 2).

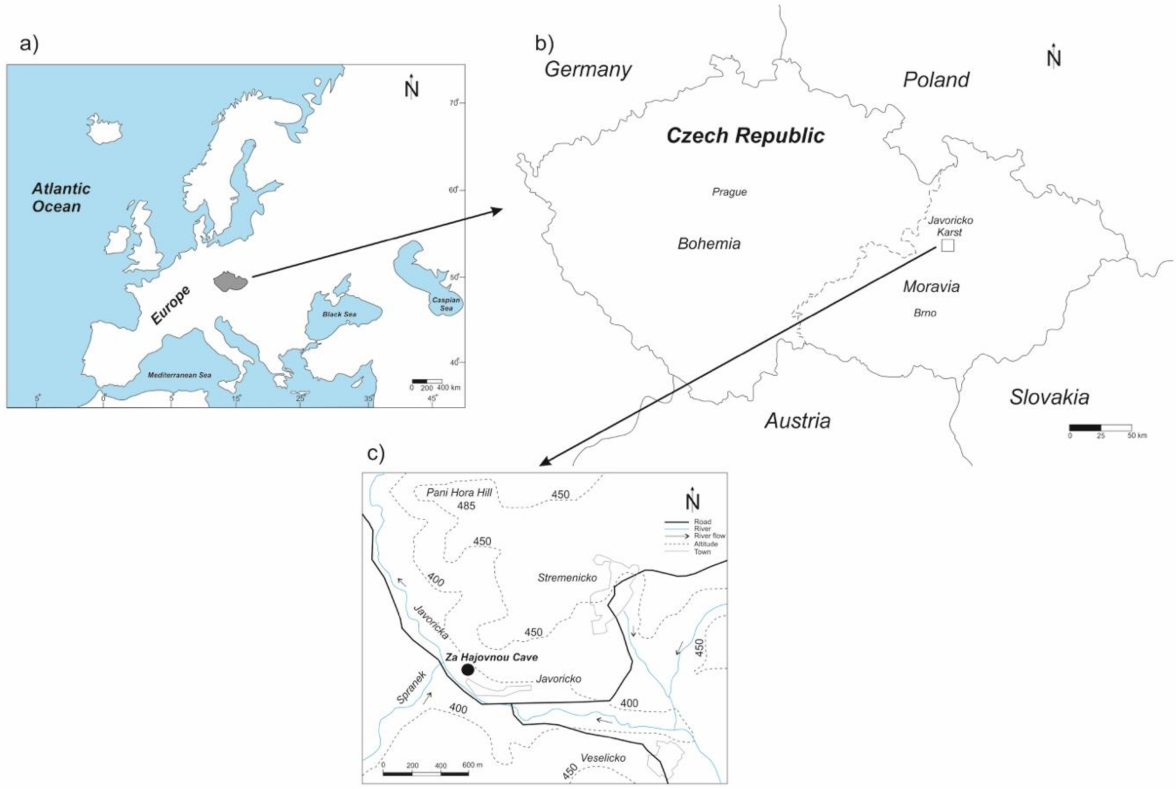

Figure 1: Location of the study area in a) Central Europe. Dashed lines in b) show more detailed placement different regions of the Czech Republic in relation to study area. Map in c) shows regional detail of the Za Hajovnou cave placement (modified after Lundberg et al., 2014; Musil, 2014).

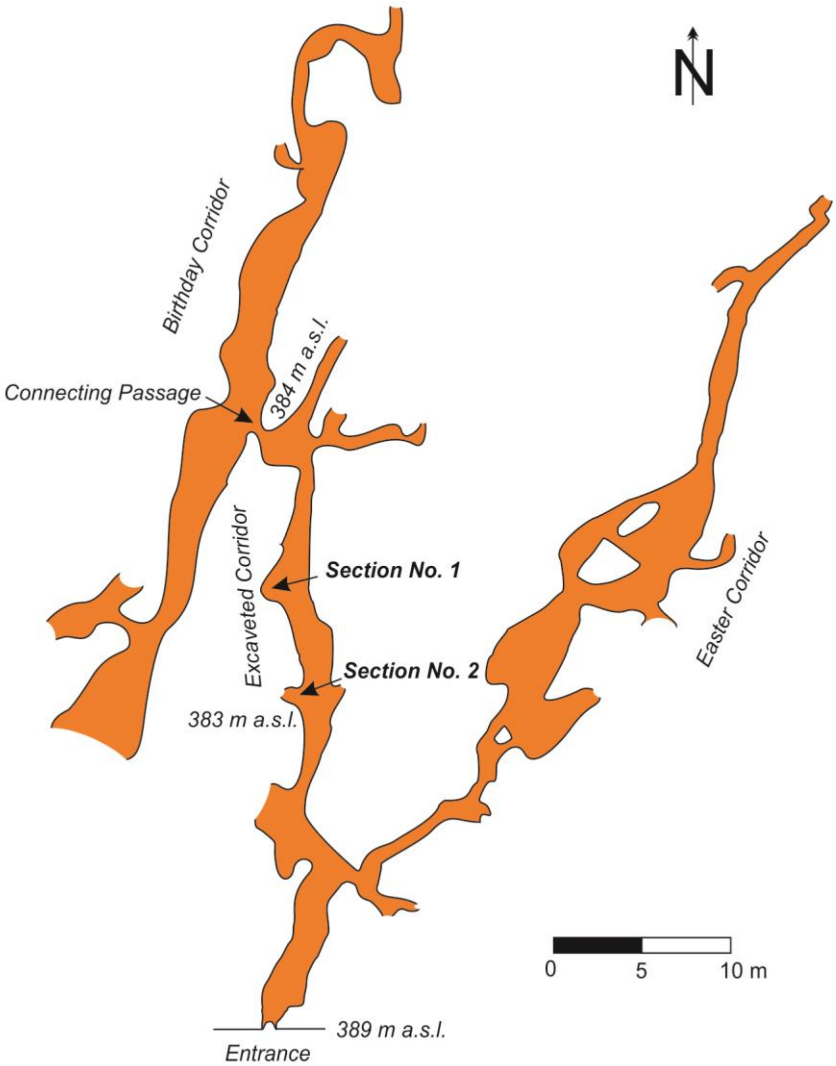

Figure 2: Map of the Za Hajovnou cave (modified after Musil, 2014; Lundberg et al., 2014; Kadlec et al., 2014). Locations marked by “Section No. 1” and “Section No. 2” is discussed in the text (Kadlec et al., 2005, 2014). Map shows relation between Connecting Passage Corridor, Birthday Corridor, and Excavated Corridor (m a.s.l.: meter above sea level).

Upper sediments of the cave were dated by U/Th dating of flowstones to 118 ± 1 to 267 ± 3 ka and by inferred Matuyama-Brunhes boundary in Section No. 1 (Figure 3) (Musil, 2005; Kadlec et al., 2005, 2014; Lundberg et al., 2014; Babek et al 2015). The sedimentation in the cave corridors were active probably from the Early Pleistocene until the beginning of the

Middle Pleistocene. The sediment then consists of Pleistocene glacial time in north-western Europe called Cromerian Interglacials complex (Muller, 1992), MIS19 (marine isotope stage) which is interglacial period ~780 ka (Pol et al., 2019) and Matuyama-Brunhes reversal (Kadlec et al. 2005, 2014; Musil et al., 2014; Musil, 2014; Zak et al., 2018; Lundberg et al., 2014).

The Matuyama-Brunhes boundary (781 ka) was suggested in the upper part of the backwater fine sediments, deposited from suspension in the flooded cave. These sediments underlay the mostly non-fluvial deposits which entered the cave through a steep passage and filled the Connecting Passage Corridor. (Kadlec et al., 2014; Lundberg et al., 2014; Musil et al., 2014).

Sedimentary sections retrieved in the Za Hajovnou cave by Kadlec et al. (2005, 2014) were composed of two parts. The first part (Section No. 1, in Figure 2) was situated in the Excavated Corridor about 28 m from the cave entrance (Kadlec et al., 2005) (Figure 2). It was intepretted to contain the magnetic transition from a reversed to a normal polarity and inferred from the age dates of the overlying non- fluvial sediments, that it could be the Matuyama-Brunhes reversal (Kadlec et al., 2005). The second sedimentary section (Section No. 2) partially overlapped the Section No. 1, and was located in the Excavated Corridor (Kadlec et al., 2014) (Figure 2). Kadlec et al. (2014) indicated that this section had sediment with just reversed polarity except upper part of the sediment where the magnetization was difficult to interpret because the sediments had weak magnetization for which the sensitivity of the Agico JR-6A spinner magnetomer was insufficient. Section No. 2 underlies the Section No. 1 and contained older backwater sediment with reversed magnetic polarity (age > 781 ka, (Kadlec et al., 2014)).

The difficulties in interpretation of the primary study by Kadlec et al. (2014) was the motivation for the presented research. Here we collected 44 oriented discrete sedimentary samples from the Excavated Corridor near the upper backwater sedimentary Section No. 1 (Figure 2, 3).

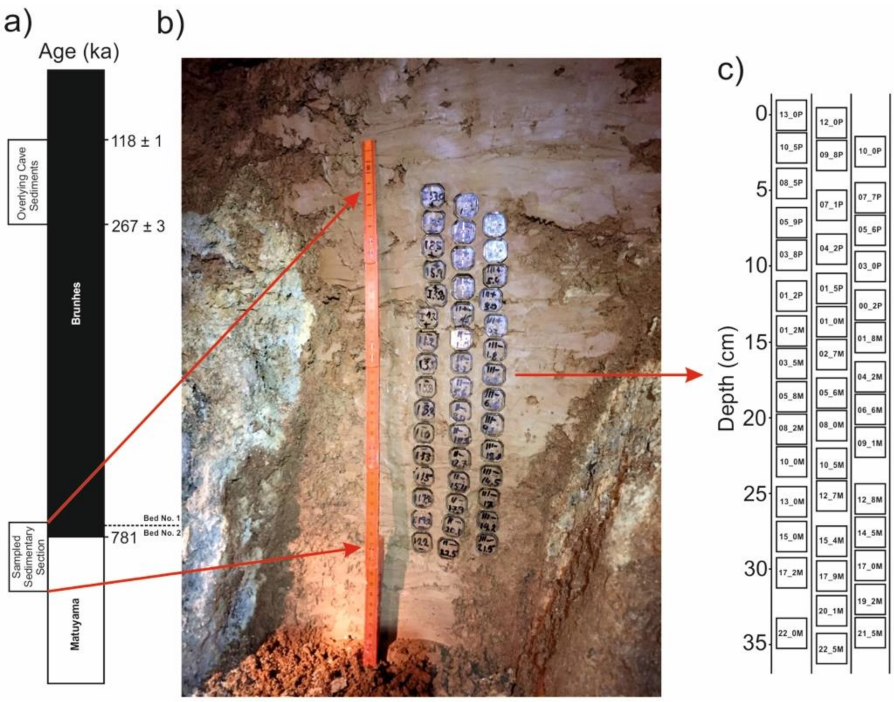

Figure 3: a) Age diagram of Za Hajovnou cave (dashed lines show the boundary between Bed No. 1 and 2 b) Sampled sedimentary Section No. 1 and c) discrete samples (numbers show the sample name).

2. Materials and Methods

2.1. Preperation of the Samples

The samples were placed in plastic boxes (2x2x2 cm; 8cc) for paleomagnetism studies. The thickness of the sampled part of the sedimentary section was 35.1 cm. Lithology of the sampled sedimentary section; The upper backwater fine sediment part was brown clayey silt with white angular clasts of weathered limestone and bone fragments (Bed No. 1) (Kadlec et al., 2014). Lower part of the section consisted of the brown silty clay without white clasts (Bed No. 2) which is presented in Figure 3 (Kadlec et al., 2014).

2.2. Demagnetization Measurements

To clean the secondary magnetizations from the sedimentary samples, we applied a stepwise alternative field (AF) demagnetization method in Pruhonice Paleomagnetism Laboratory of Czech Academy of Sciences. This method was carried out using a 2G Enterprises Cryogenic Magnetometer on 44 samples divided into 3 different sequences. The first sequence was 17 samples (13_0P, 10_5P, 09_8P, 08_5P, 05_9P, 03_8P, 01_2P, 01_2M, 03_5M, 05_8M, 08_2M, 10_0M, 13_0M, 15_0M, 17_2M, 19_2M, 22_0M) where we demagnetized at 1 mT intervals between 0-49 mT and 10 mT intervals between 50-100 mT. The second sequence was 14 samples (12_0P, 07_1P, 04_2P, 01_5P, 01_0M, 02_7M, 05_6M, 08_0M, 10_5M, 12_7M, 15_4M, 17_9M, 20_1M, 22_5M) where we demagnetized at 2 mT intervals between 0-48 mT and 10 mT intervals between 50-100 mT. The third sequence was 13 samples (10_0P, 07_7M, 05_6P, 03_0P, 00_2P, 01_8M, 04_2M, 06_2M, 09_1M, 12_8M, 14_5M, 17_0M, 21_5M) and we demagnetized at 0.5 mT intervals between 0-39.5 mT and 10 mT intervals between 40-100 mT. Demagnetization data was interpreted by using Remasoft software which was written by Agico Company (Chadima and Hrouda, 2009).

Characteristic remanent magnetization (ChRM) directions and maximum angular deviation (MAD) values were determined from principal component analysis (PCA) (Kirschvink 1980) on Zijderveld diagram (Zijderveld, 1967). Virtual geomagnetic pole's (VGP's) latitudes and longtitudes were calculated using PMGSC software by Randy Enkin. Table 1 shows the data of alternative field demagnetization for each individual sample. Two examples of alternative field demagnetization method for Matuyama and Brunhes sections of the samples with changes of declination, inclination angles and remanent magnetization intensity step by step are given in Figure 4. Rest of the samples are in the supplementary table S1 and table S2 containing supplementary Figures. Maximum angular deviation (MAD) changes of this study and comparisons with previous studies (Okada et al., 2017; Sagnotti et al., 2014) are shown in Figure 5.

Table 1: Alternative field demagnetization, virtual geomagnetic pole (VGP) data and Matuyama-Brunhes magnetic reversal scale for this study. Minus (-) values for virtual geomagnetic pole (VGP) latitudes and longtitudes indicate southern and western hemisphere. MAD: maximum angular deviation, φ_p: VGP latitude, λ_p: VGP longtitude.

Sample Name	Depth (cm)	Dec $^{(o)}$	Inc $^{(o)}$	Intensity (A/m)	MAD $^{(o)}$	φ_p (N^o/S^o)	λ_p (E^o/W^o)	
13_0P	0	369.2	65.9	7.56E-04	0.4	83.8	114.5	Brunhes
12_0P	-1	356.1	58.5	1.06E-03	1.8	79.4	-146.7	
10.5P	-2.5	379.7	37.8	8.03E-04	1.4	57.8	160.5	
10_0P	-3	407.1	44.3	7.96E-04	1.2	47	121.8	
09_8P	-3.2	401.1	33	1.04E-03	1	44.5	135.4	
08_5P	-4.5	378.5	43.2	7.02E-04	1.6	61.8	159.2	
07_7P	-5.3	378.7	25.2	7.47E-04	1.4	50.7	167.1	
07_1P	-5.9	356.1	37.3	9.54E-04	1.4	61.3	-155.8	
05_9P	-7.1	342.5	57.7	4.15E-04	1.4	73.3	-108.3	Transition
05_6P	-7.4	369.1	30.4	4.48E-04	1.1	56.1	-179.3	
04_2P	-8.8	338.7	2.1	1.01E-03	3.8	38.3	-135.9	
03_8P	-9.2	308.2	-8.4	7.45E-04	2.3	-20.2	73.2	
03_0P	-10	327.2	-32.7	1.26E-03	0.7	-16.8	49.1	
01_5P	-11.5	339.3	-15.8	6.87E-04	5.3	-29.8	40.3	
01_2P	-11.8	338.1	3.7	6.12E-04	2.6	38.9	-134.8	
00_2P	-12.8	345.3	-38.7	7.03E-04	1.3	-17.6	30.9	
01_0M	-13.6	369.6	-6.3	8.70E-04	1.4	-36.8	4.5	Matuyama
01_2M	-13.8	371.8	-21.3	5.04E-04	3.8	-28.7	3.3	

01_8M	-14.4	315.8	-49.2	1.55E-03	1.2	-1.3	53.7	
02_7M	-15.3	320.5	-22.8	8.30E-04	4.2	-19.6	57.9	
03_5M	-16.1	341.7	-33.3	5.45E-04	0.6	-20.5	35.1	
04_2M	-16.8	305.2	-40.3	7.78E-04	1.1	-2.8	65.4	
05_6M	-18.2	305.9	-32.6	5.18E-04	1.2	-7.6	67.7	
05_8M	-18.4	362.3	-61	1.06E-03	1	-1.5	-165.2	
06_6M	-19.2	282.8	-65.3	3.19E-04	3.5	-27.5	-165.4	
08_0M	-20.6	320.1	-40.3	1.25E-04	5.4	-9.4	53.3	
08_2M	-20.8	335.3	-31.6	1.37E-03	0.3	-20	41.7	
09_1M	-21.7	357.1	-58.1	1.40E-04	4.2	-1.8	18.8	
10_0M	-22.6	352.5	-66.2	1.27E-03	1.5	-8.2	-158.4	
10_5M	-23.1	393.7	-88.7	1.72E-03	1.4	-47.2	-165.6	
12_7M	-25.3	102.8	-83.7	8.05E-04	3	-50.6	177.2	
12_8M	-25.4	230.5	-72.3	8.44E-04	1.6	-59.6	-108.3	
13_0M	-25.6	299.2	-56.6	1.04E-03	0.5	-11.9	-118.2	
14.5M	-27.1	238	-68.7	9.90E-04	0.9	-54.2	-100.5	
15_M	-27.6	312	-40.3	7.71E-04	2.5	-6	60	
15_4M	-28	180.1	-89.3	8.56E-04	0.4	-50.8	-163.4	
17_0M	-29.6	234.5	-79.1	9.03E-04	0.5	-57.6	-130.3	
17_2M	-29.8	294.7	-60.7	2.11E-03	0.5	-16.9	-117.6	
17_9M	-30.5	316.8	-82.8	1.56E-03	0.7	-38.3	-151.1	
19_2M	-31.8	291.6	-87.8	4.43E-04	1.3	-47.5	-157.1	
20_1M	-32.7	256.8	-72	1.24E-03	1.5	-45.9	-113.8	
21_5M	-34.1	323.3	-23.4	3.91E-04	3.2	-20.5	55.1	

22_0M	-34.6	250.8	-61.9	2.40E-03	0.3	-42.5	-94.3	
22_5M	-35.1	143.3	-78.8	1.58E-03	0.4	-63.9	166.6	

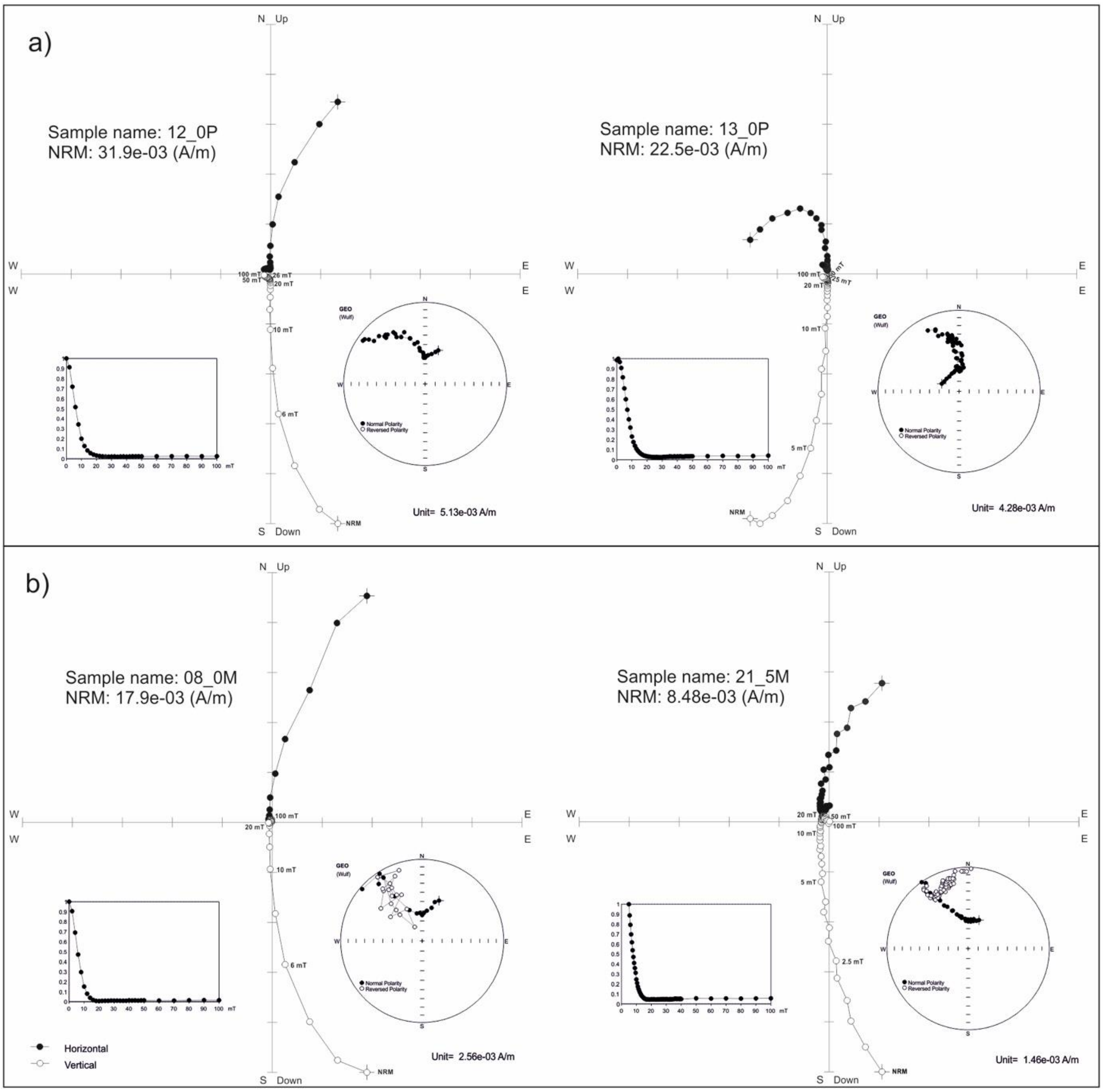

Figure 4: Changes of magnetization directions on Zijderveld diagram and Wulf stereonet during alternative field (AF) demagnetization method and demagnetization curve for typical samples (See Supplementary Figures (Table S2) for all other samples); a) normal polarity from Brunhes section (12_0P, 13_0P) and b) reversed polarity from Matuyama section (08_0M, 21_5M).

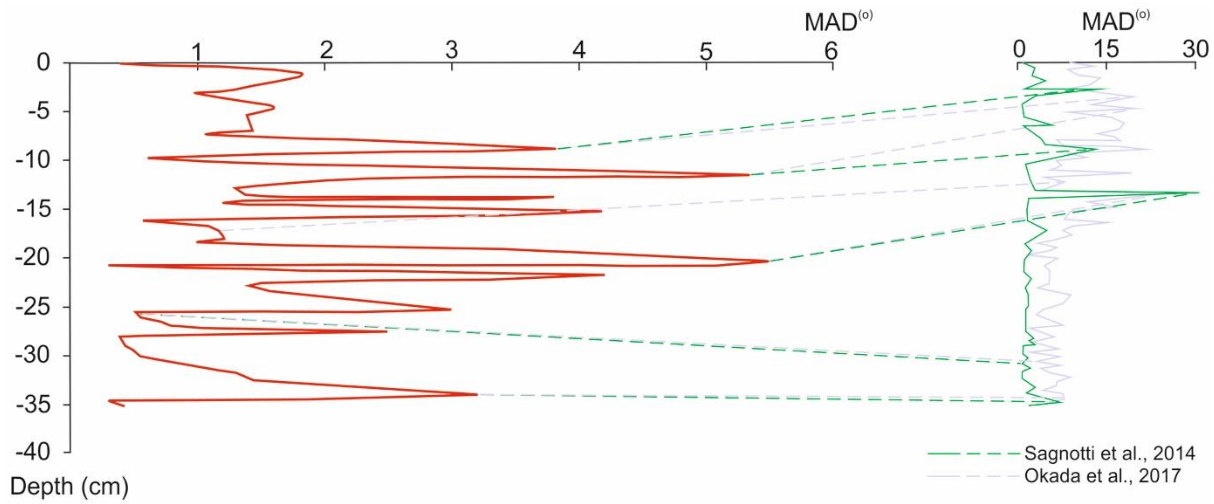

Figure 5: Comparison of Maximum angular deviation (MAD) changes from this data with published studies. during Matuyama-Brunhes magnetic reversal. Maximum angular deviation (MAD) values show error and confidence limit for this data during magnetic reversal, b: Published MAD values for datasets from Okada et al. 2017; Sagnotti et al. 2014. Colourful dashed lines connect sections published studies and this study where we see presentation of similar variation.

3. Results

3.1. Paleomagnetic Results

Sedimentary samples were demagnetized generally up to 20 mT (for details see Table S2) which removed the viscous remanent magnetization component causing change in the direction of remanent magnetization during such demagnetization for most of the samples. Intensity of the natural remanent magnetization (NRM) of the samples varies between 8.5-34.1e-3 A/m. Median destructive field (MDF) values where samples lost half of its magnetization range between 5-8 mT for the samples. NRM intensity and MDF values of the samples are shown in supplementary figures (Table S3). Maximum angular deviation (MAD) values for Matuyama and Brunhes sections are between 0.3^{o}-5.4^{o} (Figure 5). These values for transition section are between 0.7^{o}-5.3^{o} which is relatively reliable for detection of the migration of the paleomagnetic vector from a reversed to normal polarity (Figure 5). Comparisons of MAD values with previous studies (Okada et al., 2017; Sagnotti et al., 2014) shows the relative magnitude of fluctuations.

In this study, paleomagnetic data showed inclination values changing by approximately 90^{o} when measuring the sediment from 12.8 to 7.1 cm depth (Figure 6). This revealed the transition nature of the Matuyama-Brunhes magnetic reversal in Za Hajovnou cave. Below this depth, there is a Matuyama section which has inclination fluctuations between -6.3^{o}-88.7^{o} (Figure 6). Inclination angle changes between 33^{o}-65.9^{o} for Brunhes section above transition (Figure 6). Also, transition from reversed to normal polarity can be seen in declination data with similar depth (Figure 6). Despite the fluctuations, magnetic intensity values which can depend on the concentration variation of magnetic carriers of every individual sample, were decreasing for the Matuyama section from the bottom to the transition (Figure 6). After the transition from reversed to normal polarity, these values kept increasing which can be seen in Brunhes section between 7.1-0 cm depth (Figure 6). Figure 6 shows the data in comparison with other studies that consisted of various sediment types and locations around the world. Depth of the data sets was normalized considering the transition zone amd differences of sedimentation rate for each study and is not given in Figure 5, 6. Even though, there are some differencies in absolute values, comparisons of this data set with other studies showed that fluctuations and frequency of fluctuations in our data is consistent with other data sets and serves as a supporting argument for Matuyama-Brunhes magnetic reversal in Za Hajovnou cave (Figure 6).

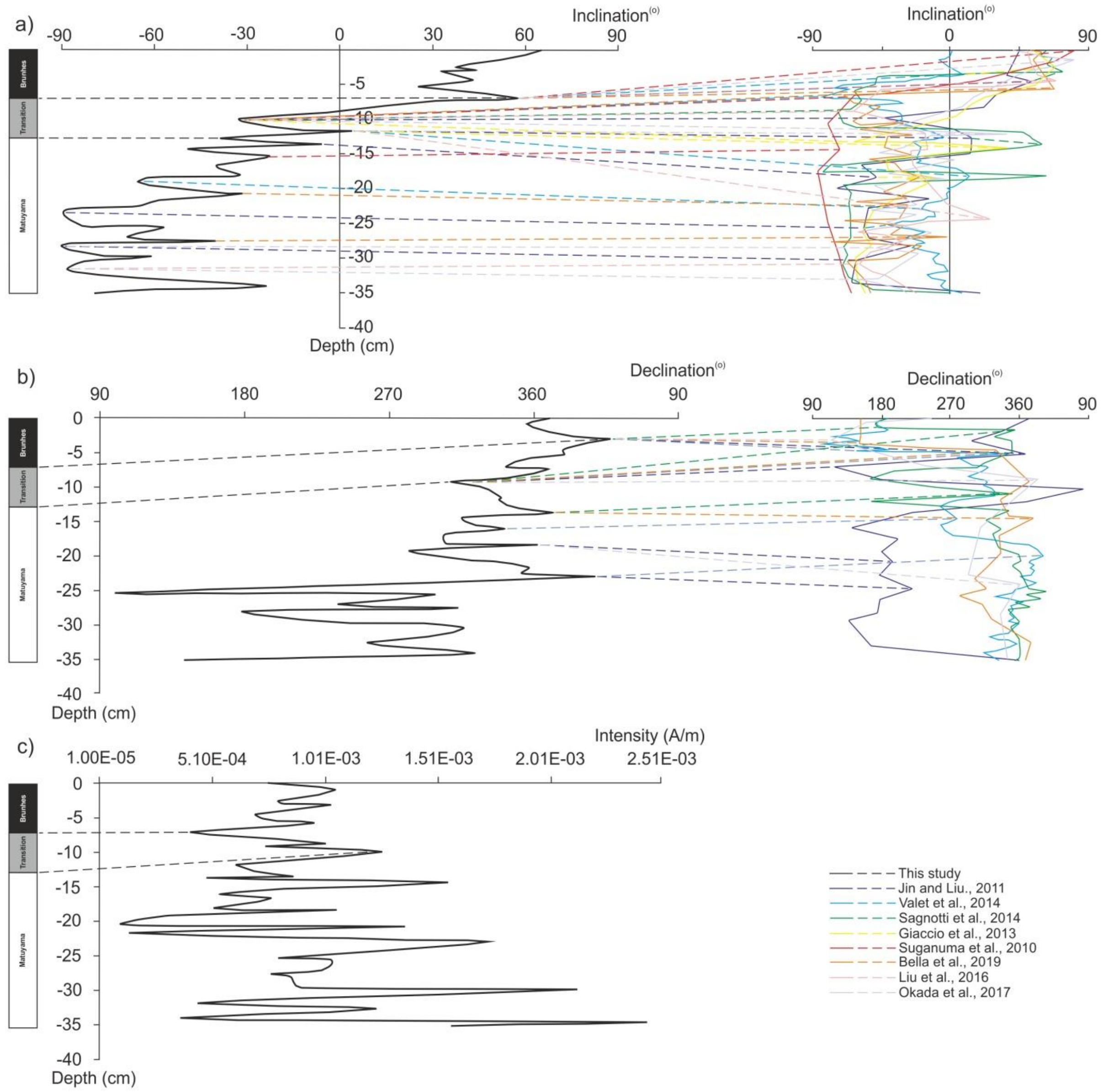

Figure 6: Comparisons of inclination and declination data with previous studies. As a result of alternative field demagnetization method, data shows a) Inclination, b) Declination and c) Magnetic intensity of the samples. Dashed lines in color connect sections published studies and this study where we see presentation of similar variation.

3.2. VGP's and Pole Migration

Virtual geomagnetic pole (VGP) shows the position of the geomagnetic paleopole (Lanza and Meloni, 2006). Virtual geomagnetic pole's (VGP) latitudes from this data set show fluctutions in Matuyama section (Figure 7). These values indicate 90^{o} change from Matuyama to Brunhes transition as a result of pole migration (Figure 7). In additon, we plotted VGP path for Matuyama, Brunhes and transition sections using VGP latitudes and longtitudes based on characteristic remanent magnetization (ChRM) directions detected in our samples (Figure 8). VGP locations for Matuyama section is in the southern hemisphere (Figure 8). During the transition from reversed to normal polarity, magnetic pole migrates from southern to northern hemisphere (Figure 8). After the geomagnetic transition, paleopoles fluctuate around geographic north pole (Figure 8). This VGP path of pole migration during the transition from the southern to northern hemisphere compares well with the Matuyama-Brunhes transition found by Okada et al. (2017) recorded in marine sediments near Japan (Figure 8).

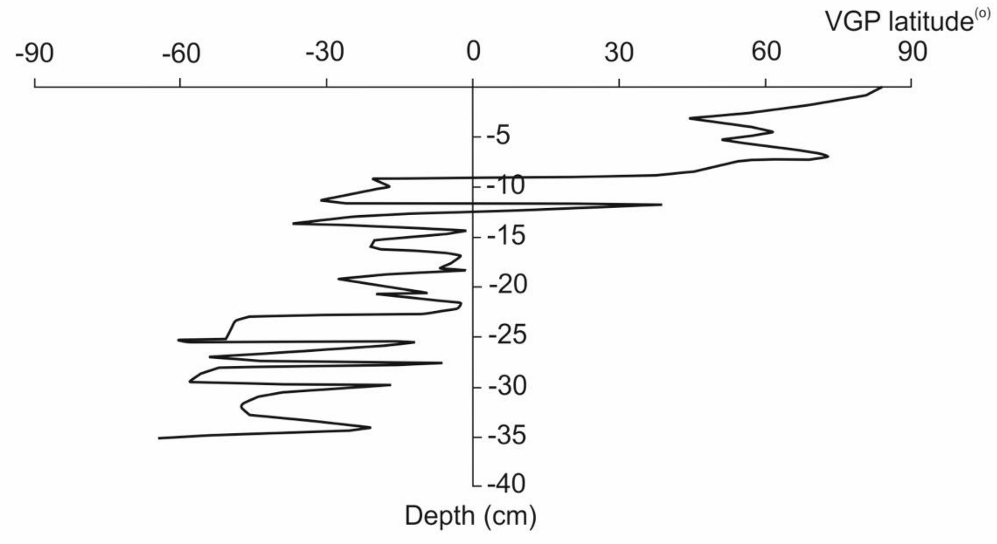

Figure 7: Virtual geomagnetic pole (VGP) latitudes for this study.

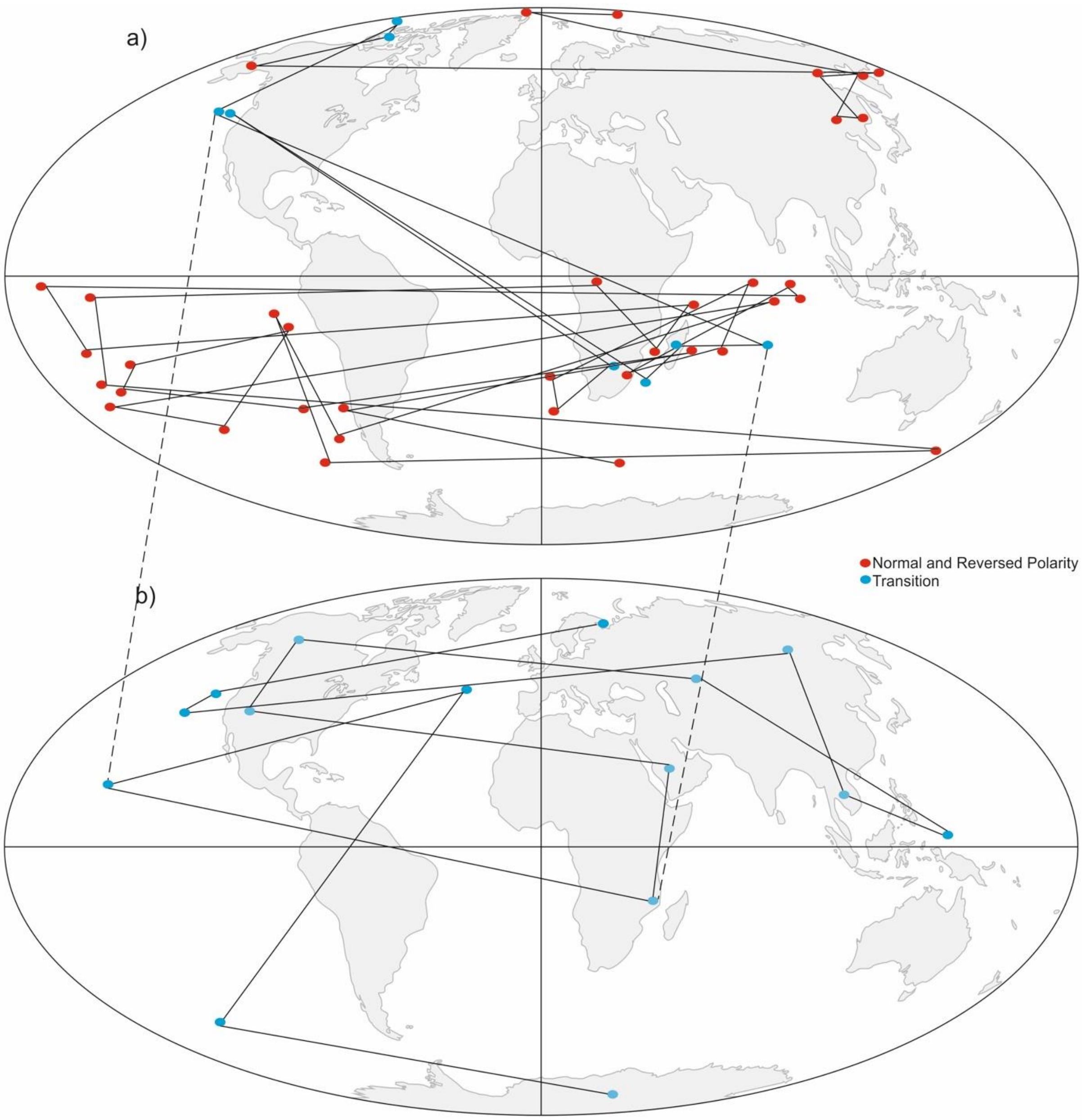

Figure 8: a) Virtual geomagnetic pole (VGP) path of this study b) VGP path of transition section from Okada et al. 2017 (dashed lines show similarities between two study).

3.3. Sedimentation Rate

Sedimentation rate of the sediment from this study in the Za Hajovnou cave is not known. We compared the thickness of transition section of our study (cm) with the thickness of transition section of other studies (cm) and estimated the sedimentation rate. Let *n* be the ratio between the two data sets which shows how thick or thin the transition section of previous study compared to our study (Equation 1.1, 1.2). This, we can estimate the sedimentation rate of Za Hajovnou (Equation 1.2). In equations, *tso* is the transition section thickness from our study (in cm), *tsp* is transition section thickness of published study (in cm), *srp* is sedimentation rate of published study (in cm/kyr), *sro* is sedimentation rate of our study (in cm/kyr).

Equations;

$$tso\ (cm)\ x\ n\ =\ tsp\ (cm) \tag{1.1}$$

$$srp\ (\mathrm{cm/kyr})/\ \mathrm{n} = sro\ (\mathrm{cm/kyr}) \tag{1.2}$$

Then, Za Hajovnou sedimentation rate ranges between 0.07-1.40 cm/kyr. Dropping the highest (1.41 cm/kyr) and lowest (0.066 cm/kyr) values gives rate between (0.2 cm/kyr – 1.0 cm/kyr) Sedimentation rate estimates are shown in Table 2 compared with other studies.

Table 2: Sedimentation rate estimations for Za Hajovnou from previous studies.

*: Sedimentation rate estimation for Za Hajovnou.

Reference	Sedimentation Rate	Sedimentation Rate*
Jin and Liu. (2011)	15 cm/kyr	0.6 cm/kyr
Okada et al. (2017)	61 cm/kyr	0.91 cm/kyr
Sagnotti et al. (2010)	61 cm/kyr	0.6 cm/kyr
Giaccio et al. (2013)	26 cm/kyr	1 cm/kyr
Sagnotti et al. (2014)	0.0224 cm/kyr	0.235 cm/kyr
Suganuma et al. (2010)	0.66 cm/kyr	0.23 cm/kyr
Bella et al. (2019)	0.64 cm/kyr	1.41 cm/kyr
Liu et al. (2016)	8.78 cm/kyr	0.066 cm/kyr

4. Discussion

Our data indicate that Matuyama Brunhes transition boundary constitutes 5.7 cm, between 7.1-12.8 cm depth of the sampled sedimentary section, of the Za Hajovnou cave sediment. Magnetic reversal is characterized by frequent fluctuations of inclination angle (Figure 6a) and VGP latitude (Figure 7). Maximum angular deviation (MAD) values of this study are within the error limit as seen in Figure 5. Similarities in comparisons of this data set with other studies indicate that Za Hajovnou cave sediment dates to Matuyama-Brunhes magnetic transition.

Because of low coercivity in most of the samples with demagnetization generally at 20 mT, some large fluctuations in the data may be considered as unstability of remanent magnetization. This shows that minerals with low coercivity is responsible for the magnetization of the cave sediments in our study. On the other hand, similar fluctuations which are seen in previous studies (Figure 6) show reliability of the data.

Although the data in this study and Okada et al. 2017 belong to geographically different locations and sediment types, this similarity during polar migration shows that the reversal was a dipole transition, and non-dipole field component was less significant (Simon et al. 2019; Mochizuki et al. 2011; Oda et al., 2000).

Our estimate of the Za Hajovnou cave's sedimentation rate seems to be significantly lower than the sediments from other studies (Jin and Liu., 2011; Okada et al., 2017; Sagnotti et al., 2010; Sagnotti et al., 2014; Giaccio et al., 2013; Suganuma et al., 2010; Bella et al., 2019; Liu et al., 2016). This is likely due to contrasting sediment types.

Analyzes of cave sediments by paleomagnetism carried out in different locations around the earth such as in Western Europe (Pares et al., 2018), South Africa (Nami et al., 2016), South America (Jaqueto et al., 2016), North America (Stock et al., 2005), Southern Europe (Pruner et al., 2010), Eastern Asia (Morinaga et al., 1992) showed that cave sediments recorded magnetic reversals. Morinaga et al. (1992) suggested low sedimentation rate for the Western Japan cave sediments 1.6 cm/kyr which shows similar rate with our Central European cave sediment estimation. King and Channel (1991) suggested that large "lock-in" depths are associated with interparticle rigidity and strength, characteristic of clayey low accumulation rate sediments (<1 cm/kyr) which results in delays of magnetic acquisition. This shows that magnetic polarity reversal could have a large (25 kyr) apparent age offset between sediments with high and very low accumulation rates (King and Channel, 1991).

Glass and Heezen (1967) claimed that a meteorite impact could result in a magnetic reversal. Large meteorite impacts may provide the sufficient moment to the exterior of the outer core to cause motion relative to the outer core. In this way, the angular difference disrupts the convection and the position of the magnetic poles. Changing in the convection pattern would affect the electric currents in the liquid core to have a new core convection with modified Coriolis forces. In addition the inner core’s angular momentum change due to the new core convection dynamics, in respect to the mantle, would change the heat transfer in the inner core and have an effet on dynamo reset. This process may cause variations in the currents producing the earth’s magnetic field and cause a geomagnetic reversal. In our study, the inclination and VGP change which have an anomaly about 12 cm depth just before the reversal (Figure 6, 7) could be a reason of a meteorite impact which was shown in a study in Indonesia from marine sediments (Hyodo et al., 2011) by micro-tektite level formed due to cosmic impacts. This can be supported with oscillations in VGP’s latitude approximately at the same depth (1.5 m) below the reversal in the study of Yamazaki and Oda (2001) in South Atlantic. Both of the studies (Hyodo et al., 2001; Yamazaki and Oda, 2001) have very similar sedimentation rates between 8-10 cm/kyr. The same anomaly can be seen in sediments from other studies (Sagnotti et al., 2014; Giaccio et al., 2013; Valet et al., 2014; Jin and Liu, 2011; Liu et al., 2016; Okada et al., 2017) (Figure 6). Migration of the pole during Matuyama polarity is towards to South America (Figure 8) which may be caused by the angular momentum and convection pattern change because of the northward directed meteorite impact in Asia (Sieh et al., 2020).

5. Conclusions

We compared the paleomagnetic data from the cave sediments with published magnetic reversal record and were able for the first time to use the detailed magnetic characteristic of cave sediment and to infer the specific magnetic reversal (Matuyama-Brunhes). This is possible due to nature of the magnetic reversal that we discovered. Note that the paleopole was residing in the east of Africa and than quickly reappeared west of North America. We consider this as an important marker signature for dating the central European paleomagnetic record from this time period.

Additionaly, we were able to design a new method for estimation of the accumulation rate of the cave sediment in Za Hajovnou cave, which until now was not known. Also we provided an evidence that a meteorite impact could be the cause of the Matuyama-Brunhes magnetic reversal.

Acknowledgements

We thank Kristina Kdyrova for their help with sample preparation and measurements and Pruhonice Paleomagnetism Laboratory for allowing to measure the cave sediment samples. Support for GK came from the Czech Science Foundation 20-08294S, 20-00892L, Ministry of Education, Youth and Sports LTAUSA 19141, and institutional support RVO 67985831.

Data Availability

Data is currently uploaded as Supplementary Information.

References

Bábek, O., Bristenský, M., Precechtìlová, G., Štìpanèíková, P., Hellstrom, J.C., Drysdale, R.N., 2015. Pleistocene speleothem fracturing in the foreland of Western Carpathians: a case study from the seismically active eastern margin of the Bohemian Massif. *Geological Quarterly*, 59 (3): 491–506. https://doi.org/10.7306/gq.1225

Bella, P., Bosák, P., Braucher, R., Pruner, P., Hercman, H., Minár, J., Veselský, M., Holec, J. and Léanni, L., 2019. Multi-level Domica–Baradla cave system (Slovakia, Hungary): Middle Pliocene–Pleistocene evolution and implications for the denudation chronology of the Western Carpathians. *Geomorphology*, *327*, pp.62-79. https://doi.org/10.1016/j.geomorph.2018.10.002

Bleil, U. and Von Dobeneck, T., 1999. Geomagnetic events and relative paleointensity records—clues to high-resolution paleomagnetic chronostratigraphies of Late Quaternary marine sediments?. In *Use of proxies in paleoceanography*(pp. 635-654). Springer, Berlin, Heidelberg.

Butler, R.F. and Butler, R.F., 1992. *Paleomagnetism: magnetic domains to geologic terranes* (Vol. 319). Boston: Blackwell Scientific Publications.

Chadima, M. and Hrouda, F., 2009. Remasoft)Paleomagnetic data browser and analyzer for Windows). Agico s.r.o.

Channell, J.E., Hodell, D.A., Singer, B.S. and Xuan, C., 2010. Reconciling astrochronological and 40Ar/39Ar ages for the Matuyama-Brunhes boundary and late Matuyama Chron. *Geochemistry, Geophysics, Geosystems*, *11*(12). https://doi.org/10.1029/2010GC003203

Giaccio, B., Castorina, F., Nomade, S., Scardia, G., Voltaggio, M. and Sagnotti, L., 2013. Revised chronology of the Sulmona lacustrine succession, central Italy. *Journal of Quaternary Science*, *28*(6), pp.545-551. https://doi.org/10.1002/jqs.2647

Glass, B. and Heezen, B.C., 1967. Tektites and geomagnetic reversals. *Nature*, *214*(5086), p.372. https://doi.org/10.1038/214372a0

Gubbins, D. and Herrero-Bervera, E. eds., 2007. *Encyclopedia of geomagnetism and paleomagnetism*. Springer Science & Business Media.

Hyodo, M., Matsu'ura, S., Kamishima, Y., Kondo, M., Takeshita, Y., Kitaba, I., Danhara, T., Aziz, F., Kurniawan, I. and Kumai, H., 2011. High-resolution record of the Matuyama–Brunhes transition constrains the age of Javanese Homo erectus in the Sangiran dome, Indonesia. *Proceedings of the National Academy of Sciences*, *108*(49), pp.19563-19568. https://doi.org/10.1073/pnas.1113106108

Jaqueto, P., Trindade, R.I., Hartmann, G.A., Novello, V.F., Cruz, F.W., Karmann, I., Strauss, B.E. and Feinberg, J.M., 2016. Linking speleothem and soil magnetism in the Pau d'Alho cave (central South America). *Journal of Geophysical Research: Solid Earth*, *121*(10), pp.7024-7039. https://doi.org/10.1002/2016JB013541

Jin, C. and Liu, Q., 2011. Revisiting the stratigraphic position of the Matuyama–Brunhes geomagnetic polarity boundary in Chinese loess. *Palaeogeography, Palaeoclimatology, Palaeoecology*, *299*(1-2), pp.309-317. https://doi.org/10.1016/j.palaeo.2010.11.011

Kadlec, J., Chadima, M., Pruner, P. and Schnabl, P., 2005. Paleomagnetic dating of sediments in the “Za Hájovnou” cave in Javoříčko - preliminary results. *Natural Studies of the Museum of the Prostějov* Region , *8* , pp.75-82.

Kadlec, J., Čížková, K. and Šlechta, S., 2014. New updated results of paleomagnetic dating of cave deposits exposed in the “Za Hájovnou” Cave, Javoříčko Karst. *Acta Musei Nationalis Pragae, Ser. B, Historia Naturalis*, *70*(1-2). https://doi.org/10.14446/AMNP.2014.27

King, J.W. and Channell, J.E., 1991. Sedimentary magnetism, environmental magnetism, and magnetostratigraphy. *Reviews of Geophysics*, *29*(S1), pp.358-370.

Kirschvink, J.L., 1980. The least-squares line and plane and the analysis of palaeomagnetic data. *Geophysical Journal International*, *62*(3), pp.699-718.

Kitaba, I., Hyodo, M., Katoh, S., Dettman, D.L. and Sato, H., 2013. Midlatitude cooling caused by geomagnetic field minimum during polarity reversal. *Proceedings of the National Academy of Sciences*, *110*(4), pp.1215-1220. https://doi.org/10.1073/pnas.1213389110

Lanza, R. and Meloni, A., 2006. *The Earth's magnetism* (Vol. 280). Springer-Verlag Berlin Heidelberg.

Liu, J., Liu, Q., Zhang, X., Liu, J., Wu, Z., Mei, X., Shi, X. and Zhao, Q., 2016. Magnetostratigraphy of a long Quaternary sediment core in the South Yellow Sea. *Quaternary Science Reviews*, *144*, pp.1-15. https://doi.org/10.1016/j.quascirev.2016.05.025

Lourens, L. J., F. J. Hilgen, J. Laskar, N. J. Shackleton, and D. Wilson. 2004. The Neogene period, in A Geologic Time Scale 2004, edited by F. M. Gradstein, J. G. Ogg, and A. G. Smith, pp. 409–440, Cambridge Univ. Press, Cambridge, U. K.

Lundberg, J., Musil, R. and Sabol, M., 2014. Sedimentary history of Za Hájovnou cave (Moravia, Czech Republic): a unique middle Pleistocene palaeontological site. *Quaternary International*, *339*, pp.11-24. https://doi.org/10.1016/j.quaint.2013.04.006

Mochizuki, N., Oda, H., Ishizuka, O., Yamazaki, T. and Tsunakawa, H., 2011. Paleointensity variation across the Matuyama-Brunhes polarity transition: Observations from lavas at Punaruu Valley, Tahiti. *Journal of Geophysical Research: Solid Earth*, *116*(B6). https://doi.org/10.1029/2010JB008093

Morinaga, H., Horie, I. and Yaskawa, K., 1992. A geomagnetic reversal recorded in a stalagmite collected in western Japan. *Journal of geomagnetism and geoelectricity*, *44*(8), pp.661-675. https://doi.org/10.5636/jgg.44.661

Muller, H., 1992. Climate changes during and at the end of the interglacials of the Cromerian Complex. In *Start of a Glacial*(pp. 51-69). Springer, Berlin, Heidelberg.

Musil, R., 2005. Jeskyně Za Hájovnou, vyjímečná lokalita Javoříčského krasu. Musil, R, pp.9-42.

Musil, R., 2014. The Unique Record Of Za Hájovnou Cave. *Acta Musei Nationalis Pragae, Series B-Historia Naturalis, 70*. https://doi.org/10.14446/AMNP.2014.7

Musil, R., Sabol, M., Ivanov, M. And Doláková, N., 2014. Middle Pleistocene Stratigraphy Of The Deposits In Za Hájovnou Cave (Javoříčko Karst, Northern Moravia, Czech Republic). *Acta Musei Nationalis Pragae, Series B-Historia Naturalis*, *70*. https://doi.org/10.14446/AMNP.2014.107

Nami, H.G., de la Pefia, P., Vásquez, C.A., Feathers, J. and Wurz, S., 2016. Palaeomagnetic results and new dates of sedimentary deposits from Klasies River Cave 1, South Africa. *South African Journal of Science*, *112*(11-12), pp.1-12. https://doi.org/10.17159/sajs .2016/20160051

Oda, H., Shibuya, H. and Hsu, V., 2000. Palaeomagnetic records of the Brunhes/Matuyama polarity transition from ODP Leg 124 (Celebes and Sulu seas). *Geophysical Journal International*, *142*(2), pp.319-338. https://doi.org/10.1046/j.1365-246x.2000.00130.x

Okada, M., Suganuma, Y., Haneda, Y. and Kazaoka, O., 2017. Paleomagnetic direction and paleointensity variations during the Matuyama–Brunhes polarity transition from a marine succession in the Chiba composite section of the Boso Peninsula, central Japan. *Earth, Planets and Space*, *69*(1), p.45. https://doi.org/10.1186/s40623-017-0627-1

Parés, J.M., Arnold, L., Duval, M., Demuro, M., Pérez-González, A., de Castro, J.B., Carbonell, E. and Arsuaga, J.L., 2013. Reassessing the age of Atapuerca-TD6 (Spain): new paleomagnetic results. *Journal of Archaeological Science*, *40*(12), pp.4586-4595. https://doi.org/10.1016/j.jas.2013.06.013

Parés, J.M., Álvarez, C., Sier, M., Moreno, D., Duval, M., Woodhead, J.D., Ortega, A.I., Campaña, I., Rosell, J., de Castro, J.B. and Carbonell, E., 2018. Chronology of the cave interior sediments at Gran Dolina archaeological site, Atapuerca (Spain). *Quaternary Science Reviews*, *186*, pp.1-16. https://doi.org/10.1016/j.quascirev.2018.02.004

Pol, K., Masson-Delmotte, V., Johnsen, S., Bigler, M., Cattani, O., Durand, G., Falourd, S., Jouzel, J., Minster, B., Parrenin, F. and Ritz, C., 2010. New MIS 19 EPICA Dome C high resolution deuterium data: Hints for a problematic preservation of climate variability at sub-millennial scale in the “oldest ice”. *Earth and planetary science letters*, *298*(1-2), pp.95-103. https://doi.org/10.1016/j.epsl.2010.07.030

Pruner, P., Hajna, N.Z., Mihevc, A., Bosák, P., Man, O., Schnabl, P. and Venhodová, D., 2010. Magnetostratigraphy and fold tests from Račiška pečina and Pečina v Borštu caves (Classical Karst, Slovenia). *Studia Geophysica et Geodaetica*, *54*(1), pp.27-48.

Sagnotti, L., Budillon, F., Dinarès-Turell, J., Iorio, M. and Macrì, P., 2005. Evidence for a variable paleomagnetic lock-in depth in the Holocene sequence from the Salerno Gulf (Italy): Implications for “high-resolution” paleomagnetic dating. *Geochemistry, Geophysics, Geosystems*, *6*(11). https://doi.org/10.1029/2005GC001043

Sagnotti, L., Cascella, A., Ciaranfi, N., Macrì, P., Maiorano, P., Marino, M. and Taddeucci, J., 2010. Rock magnetism and palaeomagnetism of the Montalbano Jonico section (Italy): evidence for late diagenetic growth of greigite and implications for magnetostratigraphy. *Geophysical Journal International*, *180*(3), pp.1049-1066. https://doi.org/10.1111/j.1365-246X.2009.04480.x

Sagnotti, L., Scardia, G., Giaccio, B., Liddicoat, J.C., Nomade, S., Renne, P.R. and Sprain, C.J., 2014. Extremely rapid directional change during Matuyama-Brunhes geomagnetic polarity reversal. *Geophysical Journal International*, *199*(2), pp.1110-1124. https://doi.org/10.1093/gji/ggu287

Sieh, K., Herrin, J., Jicha, B., Angel, D.S., Moore, J.D., Banerjee, P., Wiwegwin, W., Sihavong, V., Singer, B., Chualaowanich, T. and Charusiri, P., 2020. Australasian impact crater buried under the Bolaven volcanic field, Southern Laos. *Proceedings of the National Academy of Sciences*, *117*(3), pp.1346-1353. https://doi.org/10.1073/pnas.1904368116

Simon, Q., Suganuma, Y., Okada, M., Haneda, Y. and ASTER Team, 2019. High-resolution 10Be and paleomagnetic recording of the last polarity reversal in the Chiba composite section: Age and dynamics of the Matuyama–Brunhes transition. *Earth and Planetary Science Letters*, *519*, pp.92-100. https://doi.org/10.1016/j.epsl.2019.05.004

Stock, G.M., Granger, D.E., Sasowsky, I.D., Anderson, R.S. and Finkel, R.C., 2005. Comparison of U–Th, paleomagnetism, and cosmogenic burial methods for dating caves: implications for landscape evolution studies. *Earth and Planetary Science Letters*, *236*(1-2), pp.388-403. https://doi.org/10.1016/j.epsl.2005.04.024

Suganuma, Y., Yokoyama, Y., Yamazaki, T., Kawamura, K., Horng, C.S. and Matsuzaki, H., 2010. 10Be evidence for delayed acquisition of remanent magnetization in marine sediments: Implication for a new age for the Matuyama–Brunhes boundary. *Earth and Planetary Science Letters*, *296*(3-4), pp.443-450. https://doi.org/10.1016/j.epsl.2010.05.031

Valet, J.P., Bassinot, F., Bouilloux, A., Bourlès, D., Nomade, S., Guillou, V., Lopes, F., Thouveny, N. and Dewilde, F., 2014. Geomagnetic, cosmogenic and climatic changes across the last geomagnetic reversal from Equatorial Indian Ocean sediments. *Earth and Planetary Science Letters*, *397*, pp.67-79. https://doi.org/10.1016/j.epsl.2014.03.053

Yamazaki, T. and Oda, H., 2001. A Brunhes-Matuyama polarity transition record from anoxic sediments in the South Atlantic (Ocean Drilling Program Hole 1082C). *Earth, planets and space*, *53*(8), pp.817-827. https://doi.org/10.1186/BF03351679

Zak, K., Liptak, V., Orvosova, M., Filippi, M., Hercman, H. and Matouskova, S., 2018. Cryogenic carbonates and cryogenic speleothem damage in the Za Hájovnou Cave

(Javoříčko Karst, Czech Republic). *Geological Quarterly*, *62*(4), pp.829-839. https://doi.org/10.7306/gq.1441

Zijderveld, J.D.A., 1967. AC demagnetization of rocks: Analysis of results, Methods in Paleomagnetism DW Collinson, KM Creer, SK Runcorn, 254–286.

Additional Information

The authors declare no competing interests.